Neurocomputing 275 (2018) 1308–1317

Contents lists available at ScienceDirect

Neurocomputing

journal homepage: www.elsevier.com/locate/neucom

1-D CNNs for structural damage detection: Verification on a structural health monitoring benchmark data

Osama Abdeljaber[a], Onur Avci[a,*], Mustafa Serkan Kiranyaz[b], Boualem Boashash[b,c], Henry Sodano[d], Daniel J. Inman[d]

[a] *Department of Civil Engineering, Qatar University, Qatar*
[b] *Department of Electrical Engineering, Qatar University, Qatar*
[c] *Centre for Clinical Research, The University of Queensland, Herston, Brisbane, Australia*
[d] *Department of Aerospace Engineering, University of Michigan, Ann Arbor, MI, USA*

ARTICLE INFO

Article history:
Received 8 July 2017
Revised 17 September 2017
Accepted 22 September 2017
Available online 28 September 2017

Communicated by Jun Yu

Keywords:
Structural damage detection
Neural networks
Convolutional neural networks
Infrastructure health
Structural health monitoring
Neurocomputing
Structural damage identification

ABSTRACT

Structural damage detection has been an interdisciplinary area of interest for various engineering fields. While the available damage detection methods have been in the process of adapting machine learning concepts, most machine learning based methods extract "hand-crafted" features which are fixed and manually selected in advance. Their performance varies significantly among various patterns of data depending on the particular structure under analysis. Convolutional neural networks (CNNs), on the other hand, can fuse and simultaneously optimize two major sets of an assessment task (feature extraction and classification) into a single learning block during the training phase. This ability not only provides an improved classification performance but also yields a superior computational efficiency. 1D CNNs have recently achieved state-of-the-art performance in vibration-based structural damage detection; however, it has been reported that the training of the CNNs requires significant amount of measurements especially in large structures. In order to overcome this limitation, this paper presents an enhanced CNN-based approach that requires only two measurement sets regardless of the size of the structure. This approach is verified using the experimental data of the Phase II benchmark problem of structural health monitoring which had been introduced by IASC-ASCE Structural Health Monitoring Task Group. As a result, it is shown that the enhanced CNN-based approach successfully estimated the actual amount of damage for the nine damage scenarios of the benchmark study.

1. Introduction

Civil structures are susceptible to damage that can adversely affect their stiffness and stability, reducing their life-cycle performance. Numerous structural damage detection methods have been proposed in order to achieve an automated structural health monitoring (SHM) system capable of providing early warning against such structural damage [1–9]. Global (i.e. vibration-based) structural damage detection techniques have shown great promise in evaluating the condition of civil infrastructure [10,11], being categorized into parametric and nonparametric methods [12]. For damage identification, nonparametric global damage detection methods use statistical means to analyze the vibration response of the structure [13,14].

Recently, various machine learning algorithms have been used to develop more efficient parametric and nonparametric global damage detection techniques [15]. Structural damage detection methods based on machine learning essentially require two main steps: (1) feature extraction and (2) classification. In step 1, certain hand-crafted characteristics are extracted from the measured acceleration signals. Then, in step 2, a classifier is trained using the extracted features as inputs that are inherently mapped to the state of the structure being monitored, as the output.

In parametric machine learning based techniques, the modal parameters (damping ratios, mode shapes and frequencies) of the monitored structure are deduced from the vibration response and considered as extracted features [16]. On the other hand, nonparametric machine learning based methods implement other feature extraction techniques such as basic statistical analysis (utilizing the mean and variance of the signals) [17], autoregressive modeling [18], principal component analysis [19], wavelet transform [20] and other time-frequency methods [21]. For the classification step, several classifiers have been used in both parametric and

* Corresponding author.
E-mail addresses: o.abdeljaber@qu.edu.qa (O. Abdeljaber), oavci@vt.edu (O. Avci), mkiranyaz@qu.edu.qa (M.S. Kiranyaz), boualem.boashash@gmail.com (B. Boashash), hsodano@umich.edu (H. Sodano), daninman@umich.edu (D.J. Inman).

https://doi.org/10.1016/j.neucom.2017.09.069
0925-2312/

Notations: The following notations are used in this paper

CNN_i	1D convolutional neural network corresponding to the ith node.
DNS_i	normalized and shuffled frames for the damaged case.
D_i	output acceleration recorded by the ith accelerometer for the damaged case.
KN_i	normalized frames of the measured acceleration response.
K_i	acceleration response measured at the ith node.
PoD_{avg}	average probability of damage (i.e. overall structural score).
PoD_i	probability of damage at the ith node.
UNS_i	normalized and shuffled frames for the undamaged case.
U_i	output acceleration recorded by the ith accelerometer for the undamaged case.
N_d	the total number of frames in each damaged signal.
N_k	the total number of frames in each measured signal.
N_{l-1}	number of neurons in layer $l-1$.
$N_{r,\,i}$	the number of frames in KN_i classified by CNN_i.
N_u	the total number of frames in each undamaged signal.
b_k^l	bias to the kth neuron at layer l.
n_d	number of samples in D_i.
n_s	frame length.
n_u	number of samples in U_i.
x_k^l	input to the kth neuron at layer l.
s_i^{l-1}	output of the ith neuron at layer $l-1$.
w_{ik}^{l-1}	kernel from the ith neuron at layer $l-1$ to the kth neuron at layer l.
conv1D	1D convolution operation.
$\mathbf{D}$	measurements obtained for the fully damaged case.
$\mathbf{K}$	measured acceleration response.
$\mathbf{U}$	measurements obtained for the undamaged case.
n	number of accelerometers.

nonparametric machine learning based methods such as probabilistic neural networks (PNNs) [22,23], artificial neural networks [17], fuzzy neural networks (FNNs) [24], online sequential extreme learning machine (OS-ELM) algorithm [25], singular value decomposition [18] and support vector machine [26].

It is intuitively expected that the success of machine learning based structural damage detection techniques predominantly depends on the choice of the extracted features as well as the classifier. Therefore, the extracted features should be carefully selected so that they can capture the major characteristic condition of the analyzed signals. Also, depending on the type of extracted features, an appropriate classifier needs to be used to categorize them properly. Hence, there have been attempts to find the optimal combination of extracted features/classifier usually by trial-and-error. Yet, there is no guarantee that a particular feature/classifier combination would be the optimal choice for different structures. In other words, a certain combination found to be suitable for a particular structure may not necessarily be a good option for another. Using sub-optimal hand-crafted features and/or inappropriate classifier is likely to result in poor damage detection performance. Another problem associated with the feature extraction/classification approach is that it often needs considerable computing time and effort that prevents the utilization of machine learning techniques in vibration based structural damage detection methods for real-time SHM operations.

Recent studies have demonstrated that 1D and 2D convolutional neural networks (CNNs) can outperform conventional methods on several challenging tasks including damage detection in power engines [27], classification of electrocardiogram signals [28,29], and object recognition in images [30]. These studies, in addition to the work shown in [31–38], indicate that CNNs outperform the conventional methods not only in accuracy but also in speed. Another key feature of CNNs is their adaptive design that combines feature extraction tasks and damage classification procedure into a single learning block, allowing the CNNs simultaneously extract and learn the optimal features directly from the raw signals.

The authors have recently utilized 1D CNNs to form a nonparametric structural damage detection technique [39,40]. The success of this method to sense and locate the structural damage was tested on a steel grandstand simulator in a laboratory environment at Qatar University. The method was tested against very slight damage cases created by simply loosening some bolts at specific locations at which steel beams are connected to steel girders (connections). An individual 1D CNN was assigned to each joint of the structure. Each CNN was trained to assess the condition of its corresponding joint (i.e. to decide whether the joint is undamaged or damaged) by processing the acceleration signal measured at the joint. A large number of measurement sessions were required to generate the data needed for the CNNs training process. In the first session, the acceleration signals at all joints were measured while the structure is completely undamaged. Next, in each one of the subsequent sessions, the acceleration signals at all joints were recorded while one of the joints is damaged. Since the steel frame used in the study had 30 joints, a total of 31 measurement sessions were, therefore, conducted to collect the training data. The experimental results showed that this CNN-based damage detection algorithm was successful for identifying damaged joint(s) accurately in real-time.

The observed drawback of the CNN-based method proposed in [40] is the large number of measurement sessions needed in order to generate the required training data. This process is manageable for relatively small structures with a limited number of joints or weakness points. However, in large civil structures, it is difficult to repeat the measurement procedure for each possible damage location.

Hence, to overcome this limitation, the systematic approach presented in this paper proposes an alternative nonparametric damage detection method that utilizes 1D CNNs in a modified way. The new approach requires only two measurement sessions to obtain the training data for any structure regardless of its size. Its output is a single score which presents information on the global structural health of the structure being monitored. The success of the algorithm is assessed by utilizing the recorded data of the publicly available benchmark study, introduced by IASC-ASCE Structural Health Monitoring Task Group. The benchmark study was entitled “Experimental phase II of the structural health monitoring benchmark problem” and it was published in 2003 [41]. The aim of providing the benchmark data had been reported as to provide a unified test bed for evaluating newly developed global structural damage detection methods.

In this paper, a novel 1D CNN-based structural damage assessment approach is developed and verified using experimental data of a benchmark structural health monitoring problem. The significance of this work can be summarized as the following:

1. Unlike other machine learning based damage assessment methods available in the literature, the proposed method operates directly on the raw vibration signal without the need for preprocessing or manual feature extraction.
2. Since 1D-CNNs combine both feature extraction and classification into a single body, the proposed method is computationally

inexpensive, and therefore it can be used for real-time damage detection applications.

3. Conventional machine learning damage detection methods use hand-crafted features which are not only sub-optimal but also present a high computational complexity. On the other hand, the proposed CNN-based method uses optimal features learnt by the 1D CNNs to maximize the classification accuracy. This is the key property that improves the classification performance significantly.
4. Finally, this study introduces significant improvements to the CNN-based damage detection method in [40]. The main drawback of the method in [40] is the large number of measurement sessions required to generate training data, especially for large structures. In order to overcome this limitation, the study herein proposes an enhanced CNN-based method that requires only two measurement data sets regardless of the size of the monitored structure.

In the rest of the paper, 1D adaptive CNN implementation and training of back-propagation are summarized in Section 2. Section 3 explains the proposed systematic approach for structural damage detection algorithm. Section 4 presents the benchmark structural damage detection dataset [41] used in this study. In Section 5, the benchmark data and the associated damage cases are analyzed. In Section 6, the performance of the proposed approach is evaluated and the structural damage estimation outputs expressed in terms of *"Probability of Damage"* (PoD) scores and their correlations are discussed. Some conclusions are listed in Section 7.

2. Adaptive 1D convolutional neural networks

Through the evolution of neural networks, researchers have tried to utilize them in various useful ways to ease human life [42] including but not limited to image privacy protection [43], gesture recognition [44], speaker adaptation in automatic speech [45], auto-encoding for human pose recovery [46–49], parametrized processes [50], and active vibration control [51].

Convolutional Neural Networks (CNNs) are specific types of feed-forward artificial neural networks inspired by visual cortex of mammalians. CNNs are mainly used therefore for 2D signals such as images and video. In conventional 2D CNNs the activation function is usually either sigmoid (*sigm*), or tangent hyperbolic (*tanh*) or *ReLU* (positive linear) function. In this application where 1D CNNs have been used, the authors found out that the *tanh* activation function provided the necessary nonlinear transformations to learn such highly dynamic and noisy accelerometer signals [40].

There are two types of layers in the adaptive 1D CNNs: 1) CNN-layers where both 1D convolutions and sub-sampling occur, and 2) Multi-Layer Perceptron (MLP) layers that are very similar to the hidden and output layers of a standard MLP. Three consecutive CNN layers are illustrated in Fig. 1. They basically process the raw data and learn to extract such features that can be used by the classification performed by the MLP-layers. Therefore, both feature extraction and classification operations are fused into one body that can be optimized to maximize the classification performance. This is the main advantage of CNNs also in addition to providing a low computational complexity.

In the CNN-layers, the one-dimensional forward propagation (1D-FP) is defined by Eq. (1):

$$x_k^l = b_k^l + \sum_{i=1}^{N_{l-1}} \text{conv1D}\left(w_{ik}^{l-1}, s_i^{l-1}\right) \tag{1}$$

where:

$\boldsymbol{x_k^l}$ is defined as the input,

$\boldsymbol{b_k^l}$ is defined as the bias of the ***k*th** neuron at layer $\boldsymbol{l}$

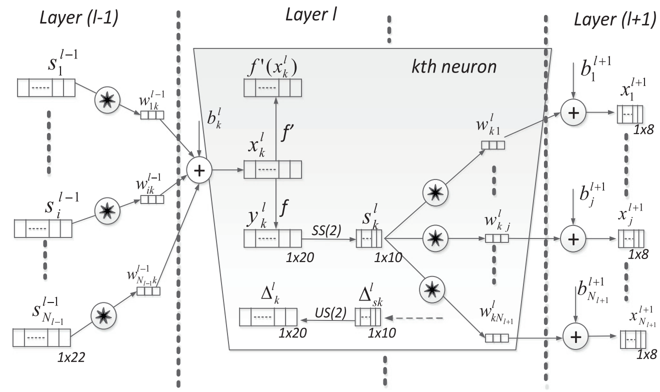

Fig. 1. The CNN layers of the adaptive 1D CNN.

$\boldsymbol{s_i^{l-1}}$ is defined as the output of the ***i*th** neuron at layer $\boldsymbol{l}-1$.

$\boldsymbol{w_{ik}^{l-1}}$ is defined as the 1D filter kernel from the ***i*th** neuron at layer $\boldsymbol{l}-1$ to the ***k*th** neuron at layer $\boldsymbol{l}$.

By this "adaptive" formulation, it is targeted that the hidden CNN layer numbers is set to any practical value since the sub-sampling factor of output CNN layer is set to its input map dimensions. Here, it must be noted that the sub-sampling factor of the output CNN layer is the hidden CNN layer just before the first MLP layer.

The training methodology, back-propagation, is briefly described in Appendix A. Further details can be found in references [29,40] and [52].

3. The proposed approach for structural damage estimation

Application of the 1D CNNs is relatively new in vibration based structural damage detection. As observed in the most current work by the authors [39,40], this method achieved an elegant damage detection and localization accuracy and promises a robust and real-time solution for SHM applications. However, as mentioned earlier, it requires significantly large amount of measurements that cannot be obtained in practice. This study proposes a systematic approach to remedy this drawback and further improve the damage estimation accuracy that will be tested over a benchmark dataset. The output of the proposed approach is a single score (out of 100%) that reflects the damage likelihood of the structure.

Consider a structure equipped with a total of n accelerometers that measure the vibration response. The first step of the proposed assessment technique is to produce data to train the 1D CNN classifiers used by this algorithm. The first set of the required data is recorded by measuring the vibration response using the n accelerometers when the structure is undamaged (i.e. the best structural condition), while the second data set is recorded when the structure is fully damaged (i.e. the worst structural condition). For example, if the purpose of the SHM system is to monitor the damage at the structural connections, the first data set should be acquired while all connections are intact, while the second set should be collected when all connections are loosened. The resulting data collected by the n accelerometers for the fully undamaged and damaged cases can be represented as

$$\mathbf{U} = \begin{bmatrix} \mathrm{U}_1 & \mathrm{U}_2 & \cdots & \mathrm{U}_n \end{bmatrix} \tag{2}$$

$$\mathbf{D} = \begin{bmatrix} \mathrm{D}_1 & \mathrm{D}_2 & \cdots & \mathrm{D}_n \end{bmatrix} \tag{3}$$

where $\mathbf{U}$ and $\mathbf{D}$ denote the measurements obtained for the undamaged and fully damaged structural cases, respectively. The terms U_i and D_i represent the output acceleration recorded by

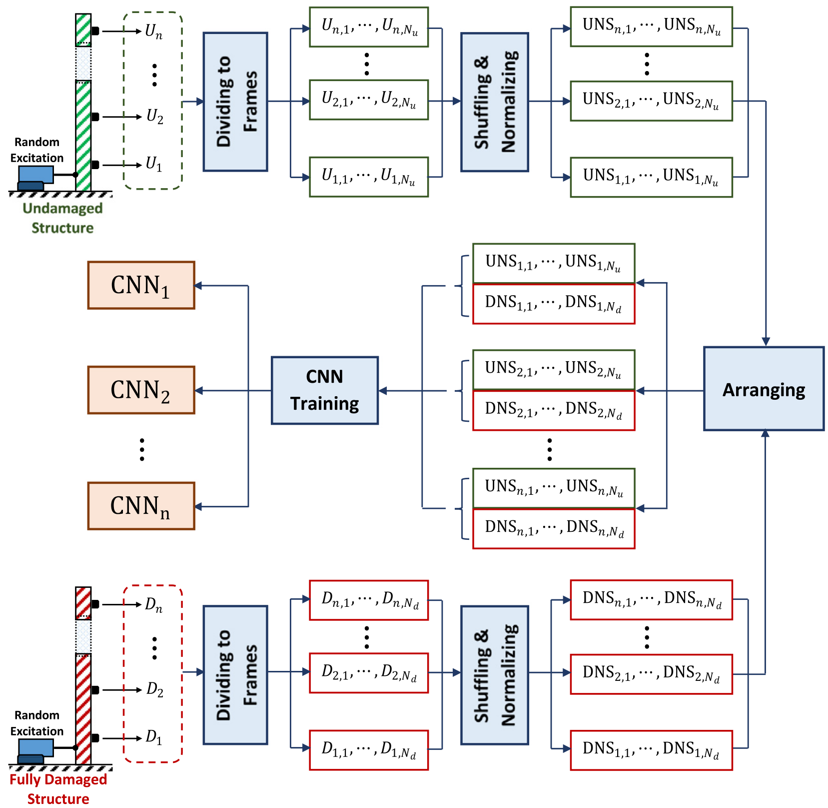

Fig. 2. The proposed data generation and CNN training process.

the ith accelerometer for the undamaged and fully damaged cases, respectively.

Assuming that each signal U_i consists of n_u samples and each signal D_i consists of n_d samples, the next step is to divide these signals into a number of frames with a fixed length n_s as follows:

$$U_i = \begin{bmatrix} U_{i,1} & U_{i,2} & \cdots & U_{i,N_u} \end{bmatrix} \tag{4}$$

$$D_i = \begin{bmatrix} D_{i,1} & D_{i,2} & \cdots & D_{i,N_d} \end{bmatrix} \tag{5}$$

where $N_u = n_u/n_s$ and $N_d = n_d/n_s$ are the total number of frames in each undamaged and damaged signal, respectively.

The next step is to train a total of n 1D CNNs (i.e. one CNN for each accelerometer). To do so, each frame in U_i and D_i is normalized between −1 and 1; then, the frames are randomly shuffled in an attempt to improve the training efficiency. The resulting normalized and shuffled vectors for the ith accelerometer can then be represented as,

$$UNS_i = \begin{bmatrix} UN_{i,1} & UN_{i,2} & \cdots & UN_{i,N_u} \end{bmatrix} \tag{6}$$

$$DNS_i = \begin{bmatrix} DN_{i,1} & DN_{i,2} & \cdots & DN_{i,N_d} \end{bmatrix} \tag{7}$$

Then, for each accelerometer i, back propagation (BP) is used to train a one dimensional CNN classifier CNN_i with normalized and shuffled frames UNS_i and DNS_i. Once the training is completed, the classifier CNN_i can classify any input frame measured at the corresponding accelerometer as fully undamaged or damaged. The data generation and CNN training process are illustrated in Fig. 2.

As mentioned earlier, the proposed method uses the resulting n CNNs to compute a single score that reflects the overall structural condition of the monitored structure. This score can be used throughout the following steps to determine whether the structure is slightly, moderately, or extremely damaged:

1. Measure the acceleration response of the monitored unit using n accelerometers. The measured signals can be written as,
$$\mathbf{K} = \begin{bmatrix} K_1 & K_2 & \cdots & K_n \end{bmatrix} \tag{8}$$
2. Each signal K_i is to be divided to a total of N_k frames each having n_s samples (i.e. the same number of samples using in the CNN training process).
$$K_i = \begin{bmatrix} K_{i,1} & K_{i,2} & \cdots & K_{i,N_k} \end{bmatrix} \tag{9}$$
3. Normalize the amplitude of the frames measured at each accelerometer i between −1 and 1.
$$KN_i = \begin{bmatrix} KN_{i,1} & KN_{i,2} & \cdots & KN_{i,N_k} \end{bmatrix} \tag{10}$$
4. The normalized frames which are measured at each accelerometer i is to be fed to CNN_i.
5. The classifier CNN_i corresponding to the ith accelerometer will process each normalized frame in KN_i and determine whether it belongs to the undamaged or to the fully damaged structural condition. Based on the classification results, the probability (in percentages) that the signal K_i belongs to the fully damaged case is computed as,
$$PoD_i = \frac{N_{r,i}}{N} \times 100 \tag{11}$$
where $N_{r,\,i}$ $(0 \le N_{r,\,i} \le N)$ represents the number of frames in KN_i classified by CNN_i as fully damaged. Therefore, low values of PoD_i (i.e. close to 0%) indicate that the signal measured at the accelerometer i belongs to the undamaged case, while high values (i.e. close to 100%) suggest that the signal belongs to the fully damaged case.
6. Finally, after computing all PoD values corresponding to the n accelerometers, the overall structural score can be obtained simply by computing the average PoD value as
$$PoD_{avg} = \frac{PoD_1 + PoD_2 + \cdots + PoD_n}{n} \tag{12}$$

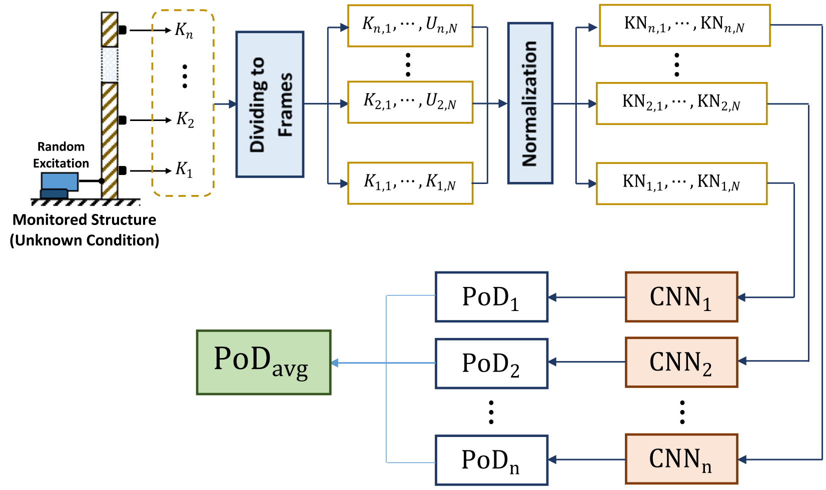

Fig. 3. Computation of PoD_{avg} value of the monitored structure using the trained CNNs.

It is expected that PoD_{avg} will reflect how close the monitored structure is to the fully damaged condition. Therefore, when the structure shows only slight deviation from normal, PoD_{avg} will be close to 0%. As the damage increases, it is anticipated that PoD_{avg} will increase gradually until it becomes very close to 100% at the fully damaged condition. The PoD_{avg} computation procedure is illustrated in Fig. 3.

4. Experimental phase II of the SHM benchmark data

Experimental phase II of the SHM benchmark problem [41] records are utilized for the study presented in this paper. The data had been put into a benchmark from and published in 2003 by the International Association for Structural Control (IASC)—American Society of Civil Engineers (ASCE) Structural Health Monitoring Task Group. The aim of providing the benchmark data was declared to provide a unified test bed for evaluating newly developed global structural damage detection methods. Compared to the Experimental Phase I benchmark problem [53], the Phase II problem includes more challenging and realistic structural damage cases [41].

The benchmark frame is a four-story steel structure built at University of British Columbia. The footprint dimensions are 2.5 m × 2.5 m and the height of the frame is 3.6 m. Two parallel steel rods were installed diagonally at each bay to provide bracing. The readers are referred to [41] for further information on the laboratory structure.

Fifteen accelerometers were placed on the structure. Starting from the ground floor, three accelerometers were installed at each level: one accelerometer at the west face; one at the east face, and another one near the central column. The sensors placed at the west and east faces were aligned to capture the accelerations along the NS direction, while the accelerometers at the central were used to record the accelerations along the EW direction.

Nine structural damage cases were simulated on the benchmark frame. For each case, acceleration output was recorded by 15 accelerometers under ambient excitation, impact hammer excitation, and 5–50 Hz randomly generated shaker excitation. As shown in Table 1 and Figs. 4 and 5, the structural damage was increased gradually from undamaged (Case 1) to very damaged in Case 9. The damage cases were introduced either by the removal of the diagonal braces at specific locations (Cases 2–7) or by bolt loosening at a number of joint locations (Cases 8 and 9).

5. Experimental results

As mentioned earlier, the acceleration measurements collected under the nine structural cases of the benchmark problem were used to test the proposed CNN-based algorithm. The data considered in this study consists of the accelerations measured at all floors except the ground floor under 5–50 Hz random shaker excitation. Therefore, the total number of accelerometers n was taken as 12. The acceleration measurements for all cases were sampled at 200 Hz. In Case 1, the vibration response was measured for 120 s, while it was measured for 300 s in Case 6 and for 360 s in the remaining cases.

As explained in Section 3, it is required to train a total of 12 CNN classifiers using only the data collected for the undamaged structural (i.e. Case 1) and the data collected while the structure is extremely damaged (i.e. Case 9). Taking the length of the frames as $n_s = 128$ samples, each one of the 12 undamaged signals of Case 1 was divided to $N_u = 187$ frames, while the 12 fully damaged signals of Case 9 were divided into $N_d = 562$ frames. Only 20% of these frames were used to train the 12 CNNs, which means that each CNN was trained using only $187 \times 0.2 = 37$ undamaged and $562 \times 0.2 = 112$ damaged frames. After normalizing and shuffling the frames as explained in Section 3, the training of 1D CNN classifiers was carried out through forward and back propagation. The CNN configuration used in this study has 2 convolutional layers, each with 15 neurons and 2 MLP layers each with 7 neurons. The kernel size was set as 41 and the sub-sampling factor was set as 2. Note that the aforementioned CNN parameters and configuration were chosen by trial-and-error.

Next, in order to test the trained CNNs, the acceleration measurements of the nine structural cases were separated into frames, and then normalized, finally fed to the corresponding CNN classifier to calculate the PoD_i at each accelerometer. Finally, computed PoD_i values were averaged to obtain the PoD_{avg} value that reflects the overall likelihood of the structure to be fully damaged. The PoD_{avg} values for all structural cases are presented in Table 2 and graphically shown in Fig. 6.

6. Discussions

The results presented in Fig. 6 show that the computed PoD_{avg} values are well correlated with the actual amount of damage induced in each structural case. For the undamaged case (i.e. Case 1), the computed PoD_{avg} value was less than 10%, which indicates that the likelihood of the structure to be fully damaged is

Table 1
Description of the structural cases in the benchmark problem [41].

Structural case	Description
1	Undamaged
2	Brace on first floor is removed in one bay on southeast corner
3	Braces on first and fourth floors are removed in one bay on southeast corner
4	Braces on all floors are removed in one bay on southeast corner
5	All east side braces are removed
6	Braces on all floors on east face are removed, and second floor braces on north face are removed
7	All braces on all faces are removed
8	Case 7 + loosened bolts on first and second floors at both ends of the beam on east face, north side
9	Case 7 + loosened bolts on all floors at both ends of beam on east face, north side

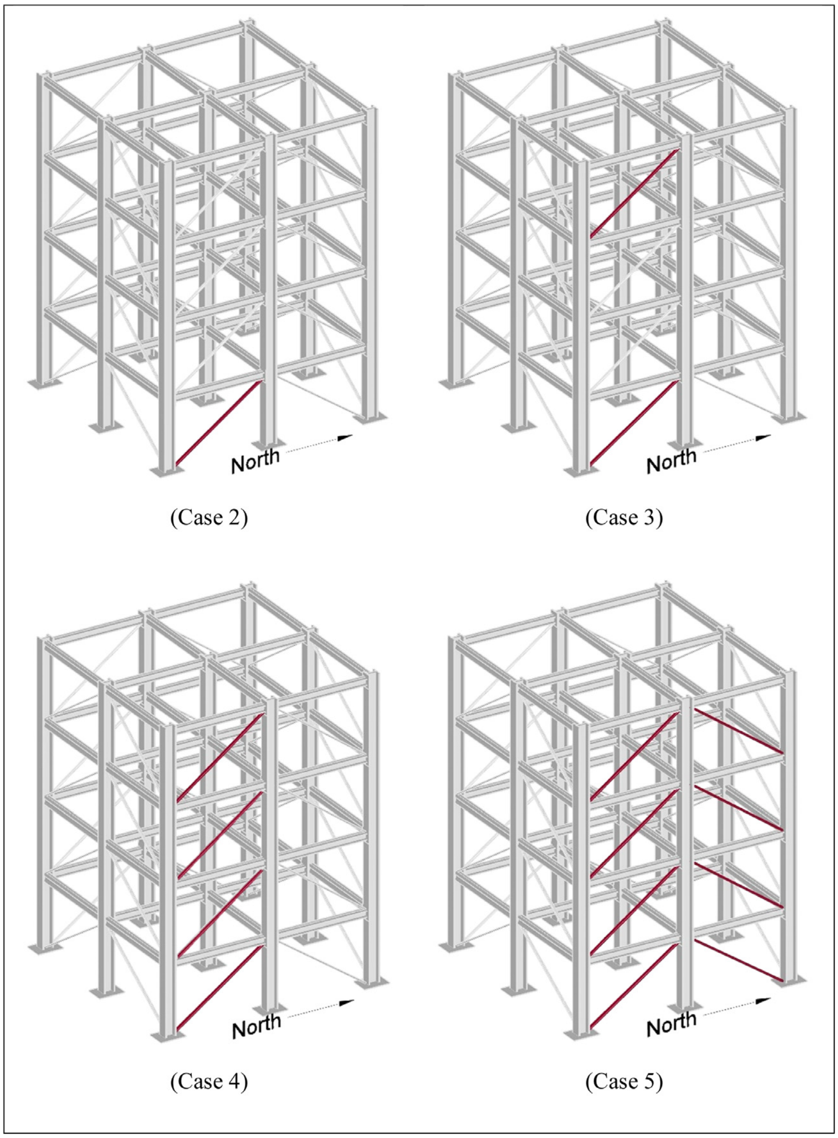

Fig. 4. Damage Cases 2 to 5 (Red color represents removed brace locations). (For interpretation of the references to color in this figure legend, the reader is referred to the web version of this article.).

negligible. Removing a single diagonal brace in Case 2 has increased the value to about 22%. As more braces were detached in Cases 3–6, the PoD_{avg} increased gradually from 27% in Case 3 to about 50% in Case 6. However, when all the remaining diagonal braces were removed in Case 7, the PoD_{avg} has significantly increased to 94%, which indicate that the structure has become very close to the fully damaged condition. Finally, with loosened bolts at number joints in Case 8 and Case 9, the PoD_{avg} has increased to almost 100%, suggesting that the structural damage has reached its peak.

Interestingly, even though the CNN classifiers were trained just by using a very small number of samples extracted from Case 1 and Case 9, they have successfully determined the amount of structural damage for all cases. In other words, although the acceleration signals of Cases 2–8 along with the remaining frames of Cases 1 and 9 were totally new to the CNNs, the algorithm was

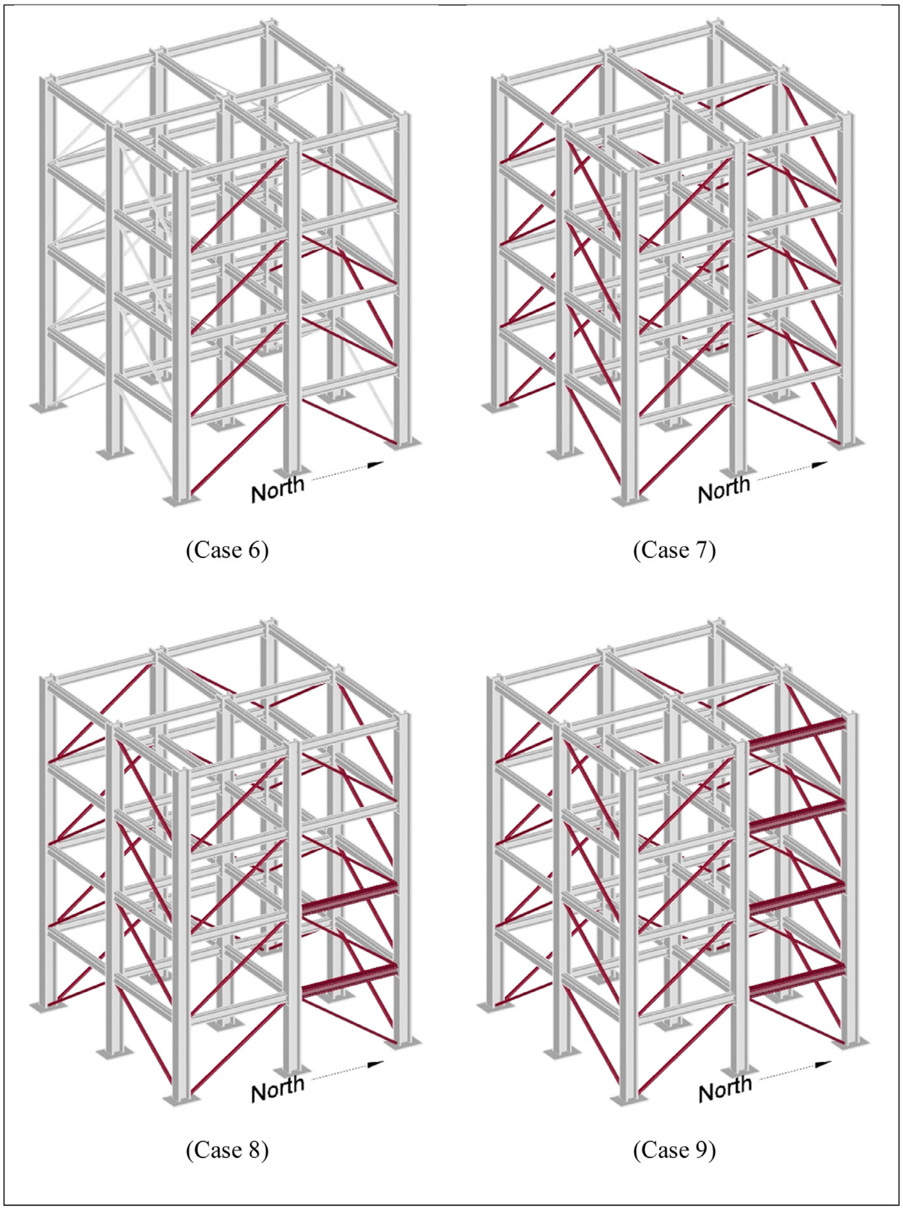

Fig. 5. Damage cases 6 to 9 (Red color represents removed brace locations or loosened beams). (For interpretation of the references to color in this figure legend, the reader is referred to the web version of this article.).

Table 2
The output of the proposed CNN-based algorithm for the nine structural cases.

Sensor ID	Sensor location	Sensor orientation	Case 1	Case 2	Case 3	Case 4	Case 5	Case 6	Case 7	Case 8	Case 9
1	1st Floor / West	N/S	4.55	40.91	15.91	63.64	20.45	16.96	95.49	96.24	100
2	1st Floor / Center	E/W	9.09	9.09	6.82	6.82	22.73	9.82	100	97.74	100
3	1st Floor / East	N/S	11.36	36.36	47.73	93.18	81.82	98.21	90.98	100	100
4	2nd Floor / West	N/S	2.27	81.82	77.27	95.45	93.18	91.96	95.49	96.99	96.99
5	2nd Floor / Center	E/W	9.09	9.09	6.82	0	4.55	4.46	100	100	100
6	2nd Floor / East	N/S	20.45	47.73	88.64	100	27.27	100	87.97	100	100
7	3rd Floor / West	N/S	11.36	0	15.91	22.73	72.73	80.36	100	100	100
8	3rd Floor / Center	E/W	18.18	11.36	20.45	11.36	0	87.5	87.22	99.25	96.99
9	3rd Floor / East	N/S	6.82	2.27	13.64	34.09	93.18	70.54	100	100	100
10	4th Floor / West	N/S	9.09	6.82	15.91	27.27	59.09	25.89	88.72	96.99	97.74
11	4th Floor / Center	E/W	13.64	20.45	9.09	6.82	9.09	4.46	100	100	100
12	4th Floor / East	N/S	2.27	0	2.27	15.91	50	14.29	86.47	86.47	95.49
PoD_{avg}			**9.85**	**22.16**	**26.71**	**39.77**	**44.51**	**50.37**	**94.36**	**97.81**	**98.93**

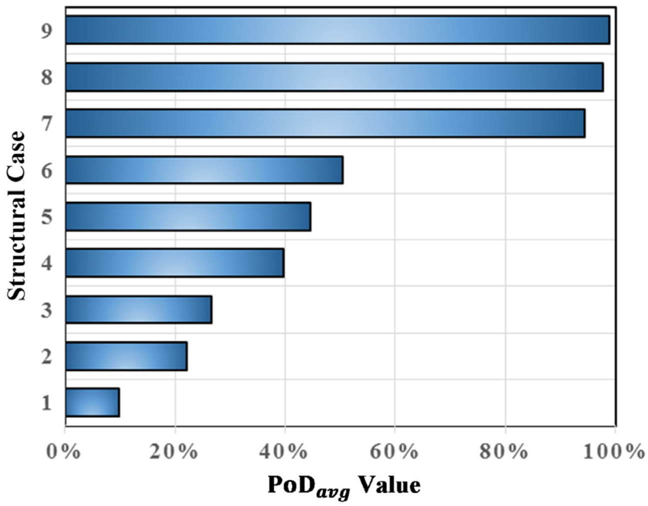

Fig. 6. Graphical representation of the PoD$_{avg}$ values computed for the nine structural cases.

successful in assigning a reasonable PoD$_{avg}$ value that reflects the actual degree of damage in all cases.

6.1. Computational complexity

The adaptive 1D CNN discussed in Section 2 was processed in C++ via C++ MSVS 2013 in 64 bit. Intel ® OpenMP API was utilized for shared memory multiprocessing. CNN training and testing were conducted on a PC with I7-4910MQ at 2.90 GHz (8 CPUs) and 32 GB memory.

A Matlab [54] code was implemented to organize, divide to frames, normalize, and shuffle the training data. As explained in Section 5, a total of 149 frames (37 undamaged frames + 112 damaged frames) were required to train each one of the 12 CNNs. Using the aforementioned implementation, the training time for each CNN ranged between 1.3 s and 8.8 s depending on the number of BP iterations. Note that the average time for a single BP iteration per frame was about 150 ms. The total training time required to train all the CNNs was about 42 s.

Similarly, another Matlab code was implemented to perform the procedure explained in Section 3. Using this code, the acceleration measurements for the nine structural cases were separated into frames, and then normalized, and finally fed into the corresponding CNN classifier to compute the PoD$_i$ at each accelerometer location. The time required to obtain the PoD$_i$ value for a 300 s acceleration signal using the corresponding CNN classifier was about 5 ms, which means that only $5 \times 12 = 60$ ms were required to get the PoD$_{avg}$ value over the 12 acceleration signals. This implies that for each 1 s of vibration monitoring, a processing time of $60/300 = 0.2$ ms was required to get PoD$_{avg}$ value which represent the general condition of the benchmark structure. This demonstrates that the overall SHM speed achieved is around 5000x faster than the “real-time” definitive requirement.

7. Conclusions

1D CNNs, which has been proven to be an efficient vibration-based structural damage detection tool by the most recent work of the authors, is tested with the data of a benchmark study in this paper. With the benchmark study data, the method simply processes the raw acceleration data measured under random excitation and compute a single score that represents the actual damage state of the monitored structure. The 1D CNN classifiers required by the algorithm were trained using a small set of acceleration samples collected in two cases: (1) when the structure is undamaged and (2) when it is fully damaged. The approach was then evaluated over the other damage cases presented in the Experimental Phase II of the SHM benchmark problem.

Following conclusions can be made based on the experimental results obtained over the benchmark data:

1. The results showed that the 1D CNN algorithm is very successful in estimating the actual amount of structural damage for the nine damage scenarios of the benchmark study.
2. The validity and efficiency of 1D CNNs in structural damage detection has been reinforced with their successful use on already existing data recorded by another research team. With that, more confidence is gained for 1D CNNs in structural damage detection applications.
3. Even though the data used for training the 1D CNNs was only collected from two structural cases (i.e. the undamaged and the fully damaged cases), the algorithm was successful in assigning reasonable scores to all separate nine structural cases considered in the study. This can be considered as a significant improvement when compared to the previous CNN-based algorithm proposed by the authors in [40], which required significant amount of data collected for training under many structural conditions. This is major and unprecedented accomplishment since it is the first system that ever achieves to detect a completely unseen damage case.
4. The CNN-based approach proposed in this paper can only be utilized to examine the overall condition of the monitored structure. As a future research topic, the possibility of utilizing the distribution of the PoD values throughout the structure to identify the location of structural damage will be investigated.
5. In some cases, it is difficult to obtain the real acceleration measurements for the fully damaged case. Therefore, in future studies, the authors will attempt to train the CNNs with real data collected under the undamaged condition together with simulated data for the fully damaged case.
6. As additional future work, the authors decided to share their own structural damage detection records as benchmark data on a public website [55].

Appendix

Back-propagation for 1D CNN

This appendix formulates the back-propagation (BP) steps without derivations. With $l = 1$ (input layer) and $l = L$ (output layer), then, the error in output layer:

$$E = \mathrm{E}\left(y_1^L, \cdots, y_{N_L}^L\right) = \sum_{i=1}^{N_L}\left(y_i^L - t_i\right)^2 \tag{13}$$

For an input vector p, and its corresponding output vector $[y_1^L, \cdots, y_{N_L}^L]$, the goal is to calculate the derivative of this error with respect to an individual weight w_{ik}^{l-1}, and bias of the neuron k, b_k^l, so that the gradient descent method can be performed to have a minimum error. Particularly, the delta of the kth neuron at layer l, Δ_k^l will be used:

$$\frac{\partial E}{\partial w_{ik}^{l-1}} = \Delta_k^l y_i^{l-1} \text{ and } \frac{\partial E}{\partial b_k^l} = \Delta_k^l \tag{14}$$

As such, the regular (scalar) back-propagation is calculated as:

$$\frac{\partial E}{\partial s_k^l} = \Delta s_k^l = \sum_{i=1}^{N_{l+1}} \frac{\partial E}{\partial x_i^{l+1}} \frac{\partial x_i^{l+1}}{\partial s_k^l} = \sum_{i=1}^{N_{l+1}} \Delta_i^{l+1} w_{ki}^l \tag{15}$$

Further back-propagation to the input delta, Δ_k^l:

$$\Delta_k^l = \frac{\partial E}{\partial y_k^l}\frac{\partial y_k^l}{\partial x_k^l} = \frac{\partial E}{\partial \mathrm{us}_k^l}\frac{\partial \mathrm{us}_k^l}{\partial y_k^l} f'\left(x_k^l\right) = \mathrm{up}\left(\Delta s_k^l\right)\beta\ f'\left(x_k^l\right) \tag{16}$$

where $\beta = (ss)^{-1}$ since each element of s_k^l is computed by averaging ss number of elements of the intermediate output, y_k^l. The inter back-propagation of the delta error ($\Delta s_k^l \xleftarrow{\Sigma} \Delta_l^{l+1}$) can be expressed as,

$$\Delta s_k^l = \sum_{i=1}^{N_{l+1}} \mathrm{conv\ 1Dz}\left(\Delta_l^{l+1},\ \mathrm{rev}\left(w_{ki}^l\right)\right) \tag{17}$$

where rev(.) is used to reverse the array and conv 1Dz(., .) is used to perform full convolution in 1D. As such, the weight and bias sensitivities can be written:

$$\frac{\partial E}{\partial w_{ik}^l} = \mathrm{conv\ 1D}\left(s_k^l, \Delta_l^{l+1}\right) \text{ and } \frac{\partial E}{\partial b_k^l} = \sum_n \Delta_k^l(n) \tag{18}$$

For more information on background and details, the readers are recommended to see [29,40] and [52].

References

[1] J.M.W. Brownjohn, Structural health monitoring of civil infrastructure, Philos. Trans. R. Soc. Math. Phys. Eng. Sci. (2007), doi:10.1098/rsta.2006.1925.

[2] S. Alampalli, M. Ettouney, Structural identification, damage identification and structural health monitoring, in: Proc. SPIE—Int. Soc. Opt. Eng., 2007, doi:10.1117/12.715000.

[3] F.N. Catbas, 1—Structural health monitoring: applications and data analysis, Struct. Health Monit. Civil Infrastruct. Syst. (2009), doi:10.1533/9781845696825.1.

[4] M. Gul, F.N. Catbas, Structural health monitoring and damage assessment using a novel time series analysis methodology with sensor clustering, J. Sound Vib. (2011), doi:10.1016/j.jsv.2010.09.024.

[5] D. Balageas, C.-P. Fritzen, A. Güemes, Structural health monitoring,, Struct. Health Monit. (2006), doi:10.1098/rsta.2006.1928.

[6] H. Sohn, C.R. Farrar, N.F. Hunter, K. Worden, Structural health monitoring using statistical pattern recognition techniques, J. Dyn. Syst. Meas. Control 123 (2001) 706–711, doi:10.1115/1.1410933.

[7] M.I. Friswell, J.E.T. Penny, Crack modeling for structural health monitoring, Struct. Health Monit. (2002), doi:10.1177/147592170200100 2002.

[8] M.W. Vanik, J.L. Beck, A Bayesian probabilistic approach to structural health monitoring, Struct. Health Monit. (1998).

[9] C.J. Stull, F.M. Hemez, C.R. Farrar, On assessing the robustness of structural health monitoring technologies, Struct. Health Monit. (2012), doi:10.1177/1475921712451956.

[10] M. Mansouri, O. Avci, H. Nounou, M. Nounou, Iterated square root unscented Kalman filter for nonlinear states and parameters estimation: three DOF damped system, J. Civil Struct. Health Monit. 5 (2015), doi:10.1007/s13349-015-0134-7.

[11] M. Mansouri, O. Avci, H. Nounou, M. Nounou, A comparative assessment of nonlinear state estimation methods for structural health monitoring, in: Conf. Proc. Soc. Exp. Mech. Ser., 2015, doi:10.1007/978-3-319-15224-0_5.

[12] O. Avci, O. Abdeljaber, Self-organizing maps for structural damage detection: a novel unsupervised vibration-based algorithm, J. Perform. Constr. Facil. (2015), doi:10.1061/(ASCE)CF.1943-5509.0000801.

[13] O. Abdeljaber, O. Avci, N.T. Do, M. Gul, O. Celik, F. Necati Catbas, Quantification of structural damage with self-organizing maps, in: Conf. Proc. Soc. Exp. Mech. Ser., 2016, doi:10.1007/978-3-319-29956-3_5.

[14] O. Abdeljaber, O. Avci, Nonparametric structural damage detection algorithm for ambient vibration response: Utilizing artificial neural networks and self-organizing maps, J. Archit. Eng 22 (2016), doi:10.1061/(ASCE)AE.1943-5568.0000205.

[15] M. Chaabane, A. Ben Hamida, M. Mansouri, H.N. Nounou, O. Avci, Damage detection using enhanced multivariate statistical process control technique, in: Proc. 2016 Seventeenth Int. Conf. Sci. Tech. Autom. Control Comput. Eng. STA 2016, 2017, doi:10.1109/STA.2016.7952052.

[16] G. Busca, A. Cigada, E. Zappa, Vision device applied to damage identification in civil engineer structures, in: Conf. Proc. Soc. Exp. Mech. Ser., 2014, doi:10.1007/978-3-319-04570-2__22.

[17] P. Chun, H. Yamashita, S. Furukawa, Bridge damage severity quantification using multipoint acceleration measurement and artificial neural networks, Shock Vib 2015 (2015).

[18] E. Figueiredo, G. Park, C.R. Farrar, K. Worden, J. Figueiras, Machine learning algorithms for damage detection under operational and environmental variability, Struct. Health Monit 10 (2011) 559–572, doi:10.1177/1475921710388971.

[19] U. Dackermann, J. Li, B. Samali, Dynamic-based damage identification using neural network ensembles and damage index method, Adv. Struct. Eng. 13 (2010) 1001–1016, doi:10.1260/1369-4332.13.6.1001.

[20] Y.-Y. Liu, Y.-F. Ju, C.-D. Duan, X.-F. Zhao, Structure damage diagnosis using neural network and feature fusion, Eng. Appl. Artif. Intell. 24 (2011) 87–92, doi:10.1016/j.engappai.2010.08.011.

[21] B. Boashash, S. Ouelha, Automatic signal abnormality detection using time-frequency features and machine learning: a newborn EEG seizure case study, Knowl.-Based Syst. 106 (2016) 38–50, doi:10.1016/j.knosys.2016.05.027.

[22] X.T. Zhou, Y.Q. Ni, F.L. Zhang, Damage localization of cable-supported bridges using modal frequency data and probabilistic neural network, Math. Probl. Eng. 2014 (2014) Article ID 837963, 10 pages, doi:10.1155/2014/837963.

[23] S.F. Jiang, C.M. Zhang, C.G. Koh, Structural damage detection by integrating data fusion and probabilistic neural network, Adv. Struct. Eng. 9 (2006) 445–458, doi:10.1260/136943306778812787.

[24] C.M. Wen, S.L. Hung, C.S. Huang, J.C. Jan, Unsupervised fuzzy neural networks for damage detection of structures, Struct. Control Health Monit. 14 (2007) 144–161, doi:10.1002/stc.116.

[25] V. Meruane, Online sequential extreme learning machine for vibration-based damage assessment using transmissibility data, J. Comput. Civil Eng. 30 (2015) 4015042, doi:10.1061/(ASCE)CP.1943-5487.0000517.

[26] A. Santos, E. Figueiredo, M.F.M. Silva, C.S. Sales, J.C.W.A. Costa, Machine learning algorithms for damage detection: Kernel-based approaches, J. Sound Vib. 363 (2016) 584–599, doi:10.1016/j.jsv.2015.11.008.

[27] T. Ince, S. Kiranyaz, L. Eren, M. Askar, M. Gabbouj, Real-time motor fault detection by 1-D convolutional neural networks, IEEE Trans. Ind. Electron 63 (2016) 7067–7075, doi:10.1109/TIE.2016.2582729.

[28] S. Kiranyaz, T. Ince, M. Gabbouj, Personalized monitoring and advance warning system for cardiac arrhythmias, Sci. Rep. 7 (2017), doi:10.1038/s41598-017-09544-z.

[29] S. Kiranyaz, T. Ince, M. Gabbouj, Real-time patient-specific ECG classification by 1-D convolutional neural networks, IEEE Trans. Biomed. Eng. 63 (2016) 664–675, doi:10.1109/TBME.2015.2468589.

[30] D. Scherer, A. Müller, S. Behnke, Evaluation of pooling operations in convolutional architectures for object recognition, in: Proc. Twentieth Int. Conf. Artif. Neural Netw. Part III, Berlin, Heidelberg, Springer-Verlag, 2010, pp. 92–101.

[31] L. Wiest, Recurrent neural networks—combination of RNN and CNN, convolutional neural networks image video process. (2017).

[32] H. Wu, X. Gu, Towards dropout training for convolutional neural networks, Neural Netw (2015), doi:10.1016/j.neunet.2015.07.007.

[33] D. Stutz, Understanding convolutional neural networks, Nips 2016 (2014), doi:10.1016/j.jvcir.2016.11.003.

[34] Y. Zhang, P. Liang, M.J. Wainwright, Convexified Convolutional Neural Networks, 2016. doi:10.1145/2951024.

[35] A. Krizhevsky, I. Sutskever, G.E. Hinton, Imagenet classification with deep convolutional neural networks, Adv. Neural Inf. Process. Syst. (2012) 1097–1105.

[36] M. Karpathy, Convolutional neural networks (CNNs/ ConvNets), CS231n Convolutional Neural Networks Vis. Recognit. (2000).

[37] A. Karpathy, G. Toderici, S. Shetty, T. Leung, R. Sukthankar, L. Fei-Fei, Large-scale video classification with convolutional neural networks, in: Large-Scale Video Classification with Convolutional Neural Networks, 2014.

[38] A. Deshpande, Understanding convolutional neural networks https://adeshpande3.github.io/adeshpande3.github.io/A-Beginner's-Guide-To-Understanding-Convolutional-Neural-Networks-Part-2/. (2014).

[39] O. Avci, O. Abdeljaber, S. Kiranyaz, D. Inman, Structural damage detection in real time: implementation of 1D convolutional neural networks for SHM applications, in: C. Niezrecki (Ed.), Structural Health Monitoring & Damage Detection, Volume 7: Proceedings of the Thirty-Fifth IMAC, A Conference and Exposition on Structural Dynamics., Springer International Publishing, 2017, pp. 49–54. Cham, 2017, doi:10.1007/978-3-319-54109-9_6.

[40] O. Abdeljaber, O. Avci, S. Kiranyaz, M. Gabbouj, D.J. Inman, Real-time vibration-based structural damage detection using one-dimensional convolutional neural networks, J. Sound Vib. 388 (2017) 154–170. http://dx.doi.org/10.1016/j.jsv.2016.10.043.

[41] S.J. Dyke, D. Bernal, J. Beck, C. Ventura, Experimental phase II of the structural health monitoring benchmark problem, in: Proc. Sixteenth ASCE Eng. Mech. Conf., 2003.

[42] Y. Guo, Y. Liu, A. Oerlemans, S. Lao, S. Wu, M.S. Lew, Deep learning for visual understanding: a review, Neurocomputing (2016), doi:10.1016/j.neucom.2015.09.116.

[43] J. Yu, B. Zhang, Z. Kuang, D. Lin, J. Fan, IPrivacy: image privacy protection by identifying sensitive objects via deep multi-task learning, IEEE Trans. Inf. Forensics Secur. (2017), doi:10.1109/TIFS.2016.2636090.

[44] E. Tsironi, P. Barros, C. Weber, S. Wermter, An analysis of convolutional long short-term memory recurrent neural networks for gesture recognition, Neurocomputing (2016), doi:10.1016/j.neucom.2016.12.088.

[45] Z. Huang, S.M. Siniscalchi, C.-H. Lee, A unified approach to transfer learning of deep neural networks with applications to speaker adaptation in automatic speech recognition, Neurocomput. Int. J. (2016), doi:10.1016/j.neucom.2016.09.018.

[46] J. Yu, C. Hong, Y. Rui, D. Tao, Multi-task autoencoder model for recovering human poses, IEEE Trans. Ind. Electron. PP (2017) 1, doi:10.1109/TIE.2017.2739691.

[47] C. Hong, J. Yu, X. Chen, Image-based 3D human pose recovery with locality sensitive sparse retrieval, in: Proc. - 2013 IEEE Int. Conf. Syst. Man, Cybern. SMC 2013, 2013, doi:10.1109/SMC.2013.360.

[48] C. Hong, X. Chen, X. Wang, C. Tang, Hypergraph regularized autoencoder for image-based 3D human pose recovery, Signal Process (2016), doi:10.1016/j.sigpro.2015.10.004.
[49] C. Hong, J. Yu, J. Wan, D. Tao, M. Wang, Multimodal deep autoencoder for human pose recovery, IEEE Trans. Image Process (2015), doi:10.1109/TIP.2015.2487860.
[50] W. Aswolinskiy, R.F. Reinhart, J.J. Steil, Modelling of parametrized processes via regression in the model space of neural networks, Neurocomputing 268 (2017) 55–63, doi:10.1016/j.neucom.2016.12.086.
[51] O. Abdeljaber, O. Avci, D.J. Inman, Active vibration control of flexible cantilever plates using piezoelectric materials and artificial neural networks, J. Sound Vib. (2016) 363, doi:10.1016/j.jsv.2015.10.029.
[52] S. Kiranyaz, T. Ince, R. Hamila, M. Gabbouj, Convolutional neural networks for patient-specific ECG classification, in: Proc. Annu. Int. Conf. IEEE Eng. Med. Biol. Soc. EMBS, 2015, doi:10.1109/EMBC.2015.7318926.
[53] J. Beck, D. Bernal, A Benchmark problem for structural health monitoring, Exp. Tech. 25 (2001) 49–52, doi:10.1111/j.1747-1567.2001.tb00026.x.
[54] MATLAB version 8.1.0.604. Natick, MA, MathWorks.
[55] A public SHM website. www.structuraldamagedetection.com.

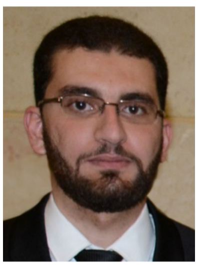

Osama Abdeljaber was born in Kuwait, 1989. He received his BS degree in Civil Engineering at Kuwait University (2011). He received his MS (2014) degree in Structural Engineering at Jordan University of Science and Technology, Irbid, Jordan. He joined Qatar University as a Research Assistant and Ph.D. student in 2014. His research interests are structural dynamics, structural health monitoring and vibration control.

Onur Avci was born in Turkey, 1979. He received his BS degree in Civil Engineering at Middle East Technical University (2000), Ankara, Turkey. He received his MS (2002) and Ph.D. (2005) degrees in Civil Engineering at Virginia Tech, Blacksburg, VA. He later worked in structural engineering firms in the United States such as Walter P Moore Associates (2005–2006); Weidlinger Associates (2006–2010) and AECOM (2010–2012) where he designed more than 4 million square feet of structural space. He joined Qatar University as an Assistant Professor in 2012. His research interests are structural dynamics, structural health monitoring and structural steel. He is a licensed professional engineer in the States of Connecticut and New York.

Serkan Kiranyaz was born in Turkey, 1972. He received his BS and MS degrees in Electrical and Electronics Department at Bilkent University, Ankara, Turkey, in 1994 and 1996, respectively. During 1996–2000 he worked as a Field Engineer in Schlumberger W&T and Senior Researcher in Nokia Research Center, Tampere, Finland. He received his Ph.D. degree in 2005 and his Docency at 2007 from Tampere University of Technology, Institute of Signal Processing respectively. He was working as a Professor in Signal Processing Department in the same university during 2009 to 2015 and he held the Research Director position for the department and also for the Center for Visual Decision Informatics (CVDI) in Finland. He currently works as a Professor in Qatar University, Doha, Qatar.

Prof. Kiranyaz published 2 books, 5 book chapters, more than 45 journal papers in 11 different IEEE Transactions and other high impact journals, and around 100 papers in international conferences. He made contributions on bio-signal analysis, particularly EEG and ECG analysis and processing, classification and segmentation, remote sensing, computer vision with applications to recognition, classification, multimedia retrieval, evolving systems and evolutionary machine learning, swarm intelligence and stochastic optimization.

Boualem Boashash, IEEE Fellow, is a scholar, professor, and senior academic with experience in five leading Universities in France and Australia. He has published more than 500 technical publications, including more than 100 journal publications covering engineering, applied mathematics, and bio-medicine. He pioneered the field of time–frequency signal processing for which he published the most comprehensive book and most powerful software package. Among many initiatives, he founded ISSPA, a leading conference since 1985. On leave from The University of Queensland, he took an appointment in the UAE as the Dean of Engineering, then moved to Qatar University as a Research Professor until 2017. His work has been cited more than 13,000 times.

Henry Sodano is a professor in the Aerospace Engineering Department at the University of Michigan with appointments in the Materials Science and Engineering and Macromolecular Science and Engineering Departments. His research lies in advanced materials with focus on composite materials, multifunctional materials, additive manufacturing, ceramics and nanotechnology. He received his Ph.D. in Mechanical Engineering from Virginia Tech in 2005, his MS in 2003 and his BS in 2002 also from Virginia Tech. He has published 220 technical articles (6 book chapters, 106 refereed journals published or submitted and 108 proceedings) and made over 100 international presentations including his selection for a presentation at the National Academy's 2008 German-American Frontiers of Engineering Symposium. He currently serves as an associate editor of four journals and was awarded the NSF CAREER award in 2009, the American Society of Composites Young Researcher Award in 2012, the ASME Gary Anderson Award for Early Career Achievement in 2009, Virginia Tech's 2010 Outstanding Recent Alumni Award, Arizona State University's 2009 Faculty Achievement Award in Research Excellence, NASA Tech Brief Awards in 2010 and 2014, and was inducted into Virginia Tech's Academy of Engineering Excellence in 2010. He is a fellow of ASME and an associate fellow of AIAA.

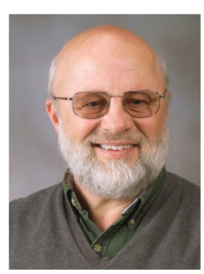

Daniel J. Inman received his Ph.D. from Michigan State University in Mechanical Engineering in 1980 and is Chair of the Department of Aerospace Engineering at the University of Michigan, as well as the C. L. "Kelly" Johnson Collegiate Professor. Since 1980, he has published eight books (on vibration, energy harvesting, control, statics, and dynamics), eight software manuals, 20 book chapters, over 350 journal papers and 600 proceedings papers, given 62 keynote or plenary lectures, graduated 62 Ph.D. students and supervised more than 75 MS degrees. He works in the area of applying smart structures to solve aerospace engineering problems including energy harvesting, structural health monitoring, vibration suppression and morphing aircraft. He is a fellow of AIAA, ASME, IIAV, SEM and AAM.